

Electromagnetic optimisation using sensitivity analysis in the frequency domain

D. Li, J. Zhu, N.K. Nikolova, M.H. Bakr and J.W. Bandler

Abstract: Gradient-based optimisation relies on the response Jacobian whose evaluation constitutes a major computational overhead in full-wave numerical analysis. Adjoint-based techniques may offer numerically efficient solutions, but their implementation is too involved in the case of full-wave computations. A simple approach that uses the self-adjoint sensitivity analysis and Broyden's update is proposed. The overhead of the Jacobian computation is greatly reduced because an adjoint system analysis is not needed and because Broyden's update is used to compute the system matrix derivatives. To improve the robustness of the Broyden update in the sensitivity analysis, we propose a switching criterion between the Broyden and the finite-difference estimation of the system matrix derivatives. We illustrate and validate the proposed method using full-wave commercial electromagnetic solvers based on the finite-element method as well as on the method of moments. Different gradient-based optimisation algorithms are exploited in the examples where efficiency is compared in terms of CPU time savings.

1 Introduction

Gradient-based optimisation is widely used to solve non-linear design and inverse-imaging problems [1–5]. It employs algorithms such as quasi-Newton, sequential quadratic programming (SQP) and trust-region methods. These algorithms exploit the objective function Jacobian and/or Hessian in addition to the objective function itself in order to search for a local optimal point. Typically, they converge much faster, that is, with significantly fewer system analyses, than algorithms utilising the objective function only (e.g. pattern search and the family of global-search algorithms). Naturally, the solution provided by a gradient-based optimisation algorithm depends on the quality of the initial design or model. And yet, because of the relatively small number of required forward solutions, gradient-based optimisation is preferred when design or inverse problems are solved with the aid of time-intensive 3-D electromagnetic (EM) simulations. The EM structure representing the starting point of the optimisation is typically the result of approximate, linearised inverse-problem solutions, equivalent-circuit designs, and so on.

The efficiency of a successful gradient-based optimisation process depends mainly on two factors: (i) the number of iterations required to achieve convergence and (ii) the number of simulation calls per iteration. The first factor depends largely on the nature of the algorithm, on the proper formulation of the objective or cost function

and on the accuracy of the response Jacobian and/or Hessian. The second factor depends on the nature of the algorithm and on the method used to compute the Jacobian and/or Hessian, which are necessary to determine the search direction and the step in the parameter space. The sensitivity analysis, which provides the Jacobian, is very time consuming when finite differences or higher order approximations are used at the response level. At least $N + 1$ full-wave simulations are needed to obtain a Jacobian for N design parameters. This is unacceptable when N is large.

It is well known that adjoint variable methods offer superior efficiency since they yield the Jacobian with only one additional (adjoint) system analysis. They have been exploited widely for design, for yield and tolerance analysis [1–4], for system stability and uncertainty analysis [5], for imaging and inverse scattering problems based on acoustic, microwave and/or near-infrared technology, and so on. In addition to [1–5], some representative examples and valuable reviews can be found in [6–10]. The adjoint variable methods have their shortcomings. A common feature in their applications is the reliance on analytical system matrix derivatives. These are not only specific to the numerical technique, but also often difficult to derive and even more difficult to implement for tasks such as shape and topology optimisation. Almost exclusively, applications are based on the finite-element method (FEM), which is relatively amenable to obtain analytical system matrix derivatives with respect to shape parameters. The major computational overhead of this adjoint-based Jacobian calculation comes from the adjoint system analysis whose computational requirements are usually comparable with those of the original system analysis.

Recently, we proposed finite-difference self-adjoint sensitivity analysis (FD-SASA) methods for the efficient computation of network parameter sensitivities, for example, the S parameters, in the frequency and time domains [11–12]. The S parameters, or functions thereof, are widely used in RF/microwave design and inverse imaging to evaluate the design or model performance and to define the objective

© The Institution of Engineering and Technology 2007

doi:10.1049/iet-map:20060303

Paper first received 2nd November 2006 and in revised form 9th April 2007

The authors are with the Department of Electrical and Computer Engineering, McMaster University, 1280 Main St. West, Hamilton, Ontario, Canada L8S 4K1

J.W. Bandler is also with Bandler Corporation, P.O. Box 8083, Dundas, Ontario, Canada L9H 5E7

D. Li and J. Zhu are currently with the Department of Electrical and Computer Engineering, University of Toronto, 10 King's College Road, Toronto, Ontario, Canada M5S 3G4

E-mail: talia@mail.ece.mcmaster.ca

function. Exploiting the self-adjoint nature of the EM problem, our method eliminates the adjoint system analysis. It yields the objective function and the Jacobian through a single EM analysis. This is a major improvement over our previous algorithms such as EM-FAST [13]. The overhead of the sensitivity analysis with the self-adjoint approach is only because of the computation of the system matrix derivatives via finite differences. It is equivalent to N matrix fills. The technique does not require any analytical pre-processing. Its only requirement is the use of the same mesh topology when the system matrices of the nominal and the perturbed structures are computed.

We have also proposed to use the Broyden update [14–15] to compute the system matrix derivatives when the Jacobian is used in an iterative optimisation loop [16–17]. Our forward solvers used in-house method of moments (MoM) codes. The feasibility of such an approach was proved and its limitation was identified – it was shown that the Broyden estimates of the system matrix derivatives may become inaccurate when the step taken in the parameter space is too small (comparable with the resolution of the discretisation grid). This drawback may inhibit convergence close to the optimal solution. The above approach is limited to in-house solvers since it needs to solve an adjoint problem. The latter is difficult to set up in the framework of a commercial EM simulator.

Here, we propose to use the Broyden-based system-matrix derivative update in conjunction with our self-adjoint formulation [11]. We refer to this approach as Broyden-update self-adjoint sensitivity analysis (B-SASA). We emphasize that, unlike FD-SASA, B-SASA is applicable only to optimisation tasks because of the iterative nature of Broyden’s formula. The big advantage of B-SASA over FD-SASA is that it has practically no computational overhead since the N additional matrix fills are unnecessary. Note that B-SASA, too, does not need an adjoint system analysis. Yet, the limitation noticed in [16–17] remains. Thus, to achieve optimal performance, we need to combine the efficiency of the B-SASA with the robustness of the FD-SASA. Here, we propose hybridisation based on a criterion for switching back and forth throughout the optimisation process between FD-SASA and B-SASA. This hybrid approach (B/FD-SASA) guarantees good accuracy of the Jacobian with minimal computational time. Also, for the first time, we show how to apply the Broyden-based sensitivity analysis with commercial solvers, both FEM and MoM based solvers. The key here is to preserve the mesh topology from one optimisation iteration to the next when B-SASA is used to compute the Jacobian. When FD-SASA is on and B-SASA is off, the mesh topology may be allowed to vary.

We validate and compare our methods using two kinds of optimisation algorithms: a minimax algorithm, which is suitable for filter and impedance-transformer design, and a least-squares algorithm, which is suitable for inverse and modelling problems. Different gradient-based search algorithms are tested such as the trust-region and the SQP. All these algorithms require the Jacobian, which is computed using the FD-SASA or the new B/FD-SASA method in separate optimisation processes. We also provide comparison with optimisation processes where the Jacobian is computed via forward finite differences directly at the response level. In the trust-region and the SQP algorithms, the Hessian is also needed but it is estimated using the classical Broyden–Fletcher–Goldfarb–Shannon (BFGS) update.

We start with a brief summary of the SASA in the FEM and the method of moments. Then, we discuss the B-SASA and the B/FD-SASA implementation in gradient-based

optimisation. Through three numerical examples, we compare the performance of the optimisation processes using the sensitivity analysis approaches discussed above.

2 Background

With a proper discretisation procedure in the frequency domain, a time-harmonic linear EM problem can be formulated as a complex system of equations

$$\mathbf{A} \cdot \mathbf{x} = \mathbf{b} \quad (1)$$

Here, $\mathbf{A} \in \mathbb{C}^{M \times M}$ is the system matrix, $\mathbf{x} \in \mathbb{C}^{M \times 1}$ is the state variable vector and $\mathbf{b} \in \mathbb{C}^{M \times 1}$ is the excitation vector, which is derived from excitation sources or inhomogeneous boundary conditions. The system matrix is a function of the vector of optimisable (shape or material) parameters $\mathbf{p} \in \mathbb{R}^{N \times 1}$, that is, $\mathbf{A}(\mathbf{p})$. Thus, the field solution vector \mathbf{x} is an implicit function of \mathbf{p} .

The SASA offers an efficient way to obtain network parameter sensitivities. It is based on the sensitivity formula (this formula assumes that the perturbation of the parameter p_n does not affect the geometry and the excitation of the port) [11]

$$\frac{\partial F}{\partial p_n} = -\hat{\mathbf{x}}^T \cdot \frac{\partial \mathbf{A}}{\partial p_n} \cdot \bar{\mathbf{x}}, \quad n = 1, \dots, N. \quad (2)$$

Here, F is a network parameter, for example, an S parameter, p_n is the n th design parameter, $\bar{\mathbf{x}}$ is solution of (1) at the current design and $\hat{\mathbf{x}}$ is the adjoint variable vector. It is the solution to the adjoint system

$$\mathbf{A}^T \cdot \hat{\mathbf{x}} = (\nabla_{\mathbf{x}} F)_{\mathbf{x}=\bar{\mathbf{x}}}^T \quad (3)$$

where $\nabla_{\mathbf{x}} F$ is the row of the derivatives of F with respect to the state variables x_i , $i = 1, \dots, M$, evaluated at $\mathbf{x} = \bar{\mathbf{x}}$. In FD-SASA, $\partial \mathbf{A} / \partial p_n$ is approximated by $\Delta_n \mathbf{A} / \Delta p_n$, where Δ_n is the finite change resulting from the perturbation Δp_n of the n th parameter alone.

In a self-adjoint problem, the adjoint solution $\hat{\mathbf{x}}$ can be expressed in terms of the original solution $\bar{\mathbf{x}}$ by multiplication with a known complex constant κ

$$\hat{\mathbf{x}} = \kappa \cdot \bar{\mathbf{x}} \quad (4)$$

For a complete network-parameter analysis of a K -port network, K full-wave simulations are performed, which yield the vectors $\bar{\mathbf{x}}_j$, $j = 1, \dots, K$. Here, the subscript indicates the port of excitation. In S -parameter analysis, for example, during each simulation, one port is excited whereas all other ports are matched. For the sensitivity of each S_{kj} , there exists a unique self-adjoint constant κ_{kj} such that $\hat{\mathbf{x}}_{kj} = \kappa_{kj} \cdot \bar{\mathbf{x}}_k$, $j, k = 1, \dots, K$ [11]. In the self-adjoint case, the sensitivity formula (2) is expressed as

$$\frac{\partial S_{kj}}{\partial p_n} = -\kappa_{kj} \cdot \bar{D}_{kj,n}, \quad n = 1, \dots, N \quad (5)$$

where

$$\bar{D}_{kj,n} = \bar{\mathbf{x}}_k^T \cdot \frac{\partial \mathbf{A}}{\partial p_n} \cdot \bar{\mathbf{x}}_j \quad (6)$$

is dependent solely on the original-system solutions, $\bar{\mathbf{x}}_j$ and $\bar{\mathbf{x}}_k$.

The complex constant κ can be derived for any EM solver if the analytical dependence of the network parameter on the field solution at the ports is known. As shown in [11],

in a finite-element solver, κ_{kj} is

$$\kappa_{kj} = \frac{1}{2\gamma_k E_{0k} \iint_{j\text{-port}} (\mathbf{a}_n \times \mathbf{E}_j^{\text{inc}}) \cdot (\mathbf{a}_n \times \mathbf{e}_j) ds_j} \quad (7)$$

Here, $\mathbf{E}_j^{\text{inc}}$ is the incident field at the j th port, \mathbf{a}_n is the unit normal to the respective port surface, \mathbf{e}_j is the normalised real vector function representing the modal E -field distribution at the j th port [18], γ_k is the modal propagation constant of the k th port and E_{0k} is a user-defined excitation magnitude for the k th port, which is usually set as 1.

In the S -parameter analysis with the MoM, κ_{kj} is given by [11]

$$\kappa_{kj} = -\frac{2Z_0}{V_e^{(k)} V_e^{(j)}} \quad (8)$$

Here, $V_e^{(j)}$ and $V_e^{(k)}$ are the j th and k th port voltage sources, respectively, usually set as 1. Z_0 is the system impedance, typically 50 Ω . Finally, if the derivatives of the input impedance Z_{in} are needed with the MoM solutions, the self-adjoint constant [11]

$$\kappa_{Z_{\text{in}}} = -I_{\text{in}}^{-2} \quad (9)$$

is used. Here, I_{in} is the complex current at the excited port computed from $\bar{\mathbf{x}}$.

In summary, using only the original system analysis, we compute the network parameters as well as their derivatives with respect to all optimisable variables. The user-defined objective function G typically depends on the network parameters analytically and its derivatives are obtained from those of the network parameters.

Finally, we note that the self-adjoint constant for a given simulation setup may also be determined empirically, that is, without any knowledge of how the network parameters depend on the field solution. The constant κ_{kj} depends only on the excitation magnitude/phase and on the modal distribution at the excited port. See, for example, (7) and (8). It is independent of the nature of the design parameters, their perturbation or the mesh setup. It is then possible to determine κ_{kj} at each frequency point of interest as the ratio of the finite difference derivative estimate with respect to any one of the design parameters and its adjoint variable counterpart. For instance, in the case of the S_{kj} parameter

$$\kappa_{kj} = \frac{\Delta_n S_{kj} / \Delta p_n}{-\bar{D}_{kj,n}}, \quad n \in \{1, \dots, N\} \quad (10)$$

where $\Delta_n S_{kj} / \Delta p_n$ is the finite difference approximation of the S_{kj} derivative at the response level obtained through parameter perturbation. The denominator is determined by the self-adjoint expression in (6).

3 Hybrid algorithm

Since in the FD-SASA, the derivatives of the system matrix are computed with a finite difference approximation, it requires at least N matrix fills. To eliminate this overhead, here, we compute the system matrix derivative applying

Broyden's formula [14] to the elements of \mathbf{A}

$$\begin{aligned} & \left(\frac{\partial \mathbf{A}}{\partial p_n} \right)^{(k+1)} \\ &= \left(\frac{\partial \mathbf{A}}{\partial p_n} \right)^{(k)} + \frac{\mathbf{A}(\mathbf{p}^{(k)} + \mathbf{h}^{(k)}) - \mathbf{A}(\mathbf{p}^{(k)}) - \sum_{j=1}^N \left(\frac{\partial \mathbf{A}}{\partial p_j} \right)^{(k)} h_j^{(k)}}{\mathbf{h}^{(k)\text{T}} \mathbf{h}^{(k)}} \\ & \quad \cdot \mathbf{h}_n^{(k)}, \quad n = 1, \dots, N \end{aligned} \quad (11)$$

$\mathbf{A}(\mathbf{p}^{(k)})$ is the system matrix at the k th iteration, when the design parameter space is $\mathbf{p}^{(k)}$, and $\mathbf{h}^{(k)}$ is the increment vector in the design parameter space between the k th and $(k+1)$ st iteration; $h_j^{(k)}$ is j th element of $\mathbf{h}^{(k)}$. The resulting sensitivity analysis algorithm is referred to as B-SASA. We note that the derivatives of the system matrix in the first optimisation iteration (when the preceding $\partial \mathbf{A}^{(0)} / \partial p_j$, $j = 1, \dots, N$, estimates are not available) are obtained with forward finite differences. In other words, the optimisation process based on B-SASA is initialised by an FD-SASA Jacobian at $\mathbf{p}^{(0)}$. The system matrix derivatives are updated iteratively thereafter. The iterative update requires negligible computational resources compared with N matrix fills.

Similar to the adjoint techniques in [16–17], where in-house MoM solvers were used for both the forward and the adjoint analyses, B-SASA requires that the discretisation mesh remains of the same topology from one optimisation iteration to the next. This preserves the size of the system matrix as well as the numbering of the mesh nodes and mesh edges.

The derivatives of the Broyden update are less accurate than those in the FD-SASA. The inaccuracy tends to be significant when the increment of the design parameters is very small, for example, near a local minimum, as catastrophic cancellation occurs. We propose two criteria to switch from B-SASA to FD-SASA: $G(\mathbf{p}^{(k)}) > G(\mathbf{p}^{(k-2)})$ and $\|\mathbf{h}_k\| \leq d$. Here, G is the objective function (defined through the network parameters) and d is the minimum edge length of the mesh elements. In effect, the first criterion checks for possible divergence because of inaccurate Jacobian, whereas the second criterion checks whether the step taken in the shape-parameter space has become smaller than the resolution of the numerical grid. The algorithm checks the two criteria at every iteration. If either one or both criteria are satisfied, a switch from B-SASA to FD-SASA occurs – the forward solver is allowed to re-mesh the structure completely and the Jacobian is computed with FD-SASA. After a switch occurs, only one optimisation iteration is performed with the FD-SASA Jacobian, after which the algorithm returns to B-SASA. This B/FD-SASA method is simple and guarantees acceptable accuracy of the system matrix derivatives even for small increments in the design parameter space.

4 Numerical results

We perform gradient-based optimisation using the response Jacobian provided by: (i) the proposed hybrid B/FD SASA approach, (ii) the FD-SASA and (iii) the forward finite difference approximation at the response level denoted by FD. We compare the performance of the optimisation algorithm with the three sensitivity analysis approaches in terms of number of iterations and the overall CPU time.

4.1 Validation with the FEM

We validate our algorithm with a FEM solver FEMLAB [19] by two numerical examples: an H-plane waveguide filter and an inverse imaging problem.

4.1.1. H-plane waveguide filter: The six-section H-plane filter is shown in Fig. 1 [20]. The rectangular waveguide is of width 3.485 cm and height 1.58 cm. The cut-off frequency of the TE₁₀ mode is 4.3 GHz. The six resonators are separated by seven septa of finite thickness $\delta = 0.625$ mm. The design parameters are the resonator lengths L_1, L_2 and L_3 , and the septa widths W_1, W_2, W_3 and W_4 . A minimax objective function is used with the design specifications

$$\begin{aligned} |S_{21}| &\leq 0.52 & \text{for } f \leq 5.0 \text{ GHz} \\ |S_{21}| &\geq 0.98 & \text{for } 5.5 \leq f \leq 9.0 \text{ GHz} \\ |S_{21}| &\leq 0.7 & \text{for } \geq 9.5 \text{ GHz.} \end{aligned} \quad (12)$$

We choose 12 uniformly distributed points in the frequency range from 4.5 to 10.0 GHz. The initial design is given by $\mathbf{p}^{(0)} = [L_1 \ L_2 \ L_3 \ W_1 \ W_2 \ W_3 \ W_4]^T = [12 \ 14 \ 18 \ 14 \ 11 \ 11 \ 11]^T$ (all in mm). Its $|S_{21}|$ response is plotted in Fig. 2.

We use Madsen's minimax optimisation algorithm [21], which employs a trust region, and the Matlab minimax algorithm, which employs SQP. We refer to these algorithms as TR-minimax and SQP-minimax, respectively. For TR-minimax, the initial trust-region radius is set to $r_0 = 0.03 \cdot \|\mathbf{p}^{(0)}\|_2$. Generally, the choice of the initial trust region radius depends on the nonlinearity of the objective function at the initial point [22]. Many algorithms use an ad hoc value and the user is expected to provide an initial guess. This is the case with this particular optimisation code. The value above was chosen so that it is sufficiently smaller than $0.1 \cdot \|\mathbf{p}^{(0)}\|_2$ – a value recommended for a weakly nonlinear problem – since from previous experience we know that the H-plane filter design problem is strongly nonlinear. We point out that there exist fully automated approaches to determining the initial trust region radius, which exploit the response and/or the Jacobian, the Jacobian norm or the distance to the Cauchy point at $\mathbf{p}^{(0)}$ [22, 23]. For example, Matlab's fmincon algorithm, which employs a trust region, computes the initial trust region radius automatically. We use this algorithm in our second example.

We use the FD-SASA, the B/FD-SASA and the FD to supply the Jacobian in three separate optimisation processes. The response Jacobian is calculated at all 12 frequency points of interest. Note that each of these Jacobians is a continuous function in the design parameter space

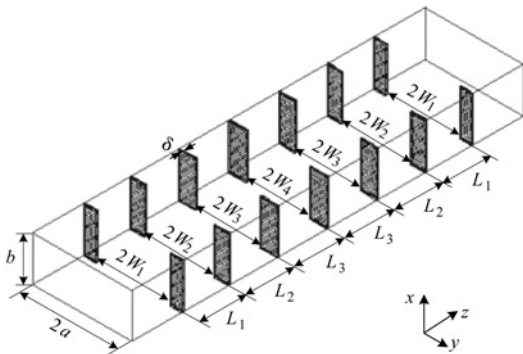


Fig. 1 Six-section H-plane filter

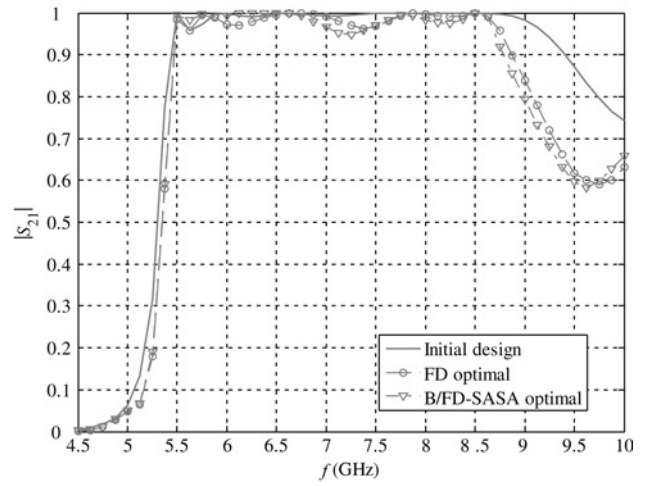


Fig. 2 Insertion loss of the initial and the optimised H-plane filter designs

although the Jacobian of the minimax objective function is not. The minimax optimisation algorithms operate with the complete set of Jacobians.

Figs. 3 and 4 show the parameter step size and the objective function against the iterations in the TR-minimax optimisation with all three sensitivity analysis techniques. Figs. 5 and 6 illustrate the same three cases with SQP-minimax. In Table 1, the optimal designs achieved by the three TR-minimax approaches are compared.

Table 2 shows the number of iterations and the time cost of the three optimisation processes. We notice in Table 2 that SQP-minimax takes longer than TR-minimax despite the smaller number of iterations. This is because of SQP-minimax may call for a system analysis several times per iteration in order to determine the next step in the parameter space. TR-minimax needs only one system analysis per iteration.

One FEM simulation (full-frequency sweep) of the structure takes ~ 43 s. One system analysis (full-frequency sweep) involves obtaining the S_{21} parameter and its seven derivatives with respect to the design parameters. To accomplish this, eight FEM simulations are necessary using the FD sensitivity analysis (~ 344 s per system analysis). As Table 2 shows, TR-minimax with FD sensitivities takes 11 iterations to converge. The simulation time ($11 \times 344 = 3784$ s) accounts for almost all of the total time of the optimisation process, which is ~ 3825 s. The

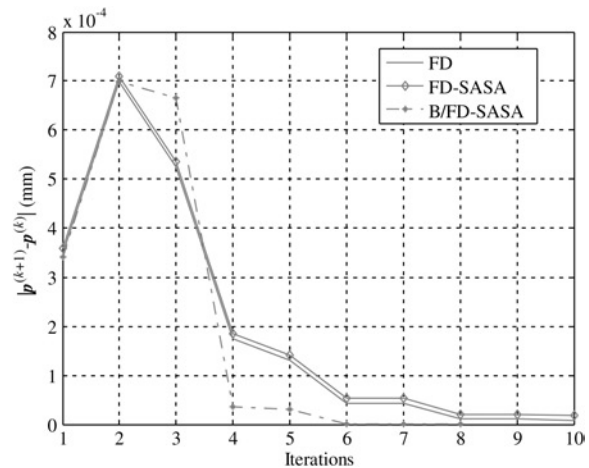


Fig. 3 Parameter step size against optimisation iterations in the TR-minimax optimisation of the H-plane filter

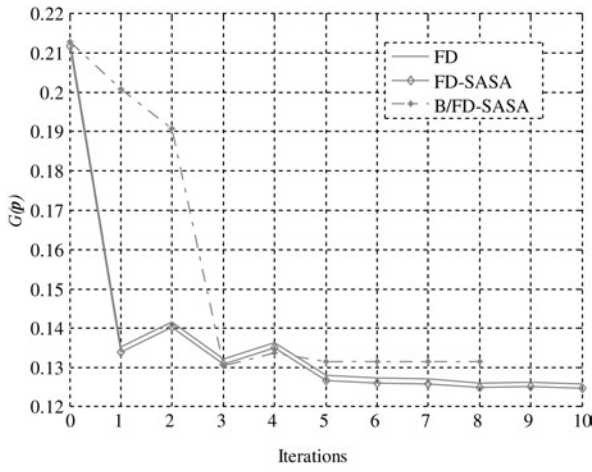


Fig. 4 Objective function against optimisation iterations in the TR-minimax optimisation of the H-plane filter

remaining difference of ~ 40 s accounts for data transfer and the calculations of the optimisation algorithm. Within this time, the total overhead associated with the FD estimation of the seven derivatives is ~ 3311 s, that is, the overhead per system analysis is 301 s. This derivative estimation overhead is reduced to 172 s in FD-SASA, whereas in B-SASA it is 44 s. We note that in the TR-minimax optimisation process, the B/FD-SASA method switches from B-SASA to FD-SASA once at the 5th iteration. Thus, the Jacobian estimation time (524 s) includes one FD-SASA computation and eight B-SASA computations. With SQP-minimax, B/FD-SASA does not switch and only B-SASA is invoked in the Jacobian calculation. The optimal points of the different methods are practically the same and so are their responses (see Fig. 2).

The reduction in the overhead of the sensitivity calculation as well as the overall time of the optimisation process with B/FD-SASA becomes increasingly pronounced as the size of the system matrix and the number of optimisable parameters increase.

4.1.2 2-D inverse problem: The 2-D inverse imaging problem is shown in Fig. 7. The lossy inhomogeneous structure is illuminated by a TEM wave for frequencies from 5 to 9 GHz with an interval of 0.5 GHz. The objective is to determine the position and size of an object immersed in

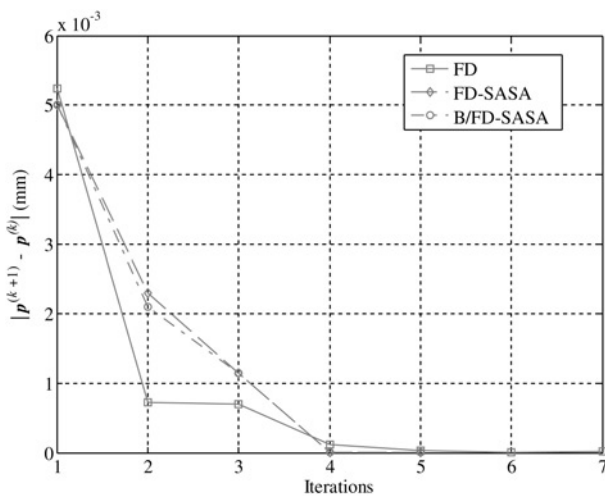


Fig. 5 Parameter step size against optimisation iterations in the SQP-minimax optimisation of the H-plane filter

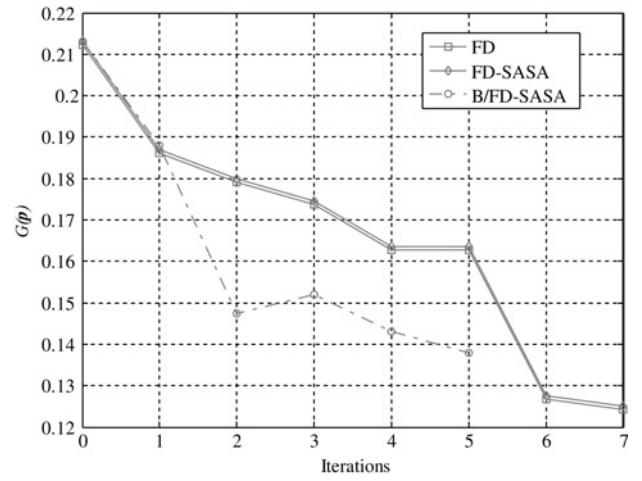


Fig. 6 Objective function against optimisation iterations in the SQP-minimax optimisation of the H-plane filter

the host medium. The object is modelled as a rectangular area with width w and length l . The distance to the interface is d . The object has a relative permittivity $\epsilon_{r2} = 45$ and specific conductivity $\sigma_2 = 4.5$. The host medium is characterised by $\epsilon_{r1} = 12$ and $\sigma_1 = 0.5$. The computational domain is surrounded by absorbing boundaries. To obtain a target response, we perform a simulation with the target shape parameters $\bar{\mathbf{p}} = [w \ l \ d] = [44 \ 55 \ 5]$ (in mm). The target response is the magnitude of the reflection coefficient, $|\bar{S}_{11}|$.

We optimise the three shape parameters so that the simulated response matches the target response. The least-squares objective function is

$$G(\mathbf{p}) = \sqrt{\sum_{i=1}^9 [|S_{11}(\mathbf{p}, f_i) | - |\bar{S}_{11}(f_i) |]^2} \quad (13)$$

Here, $|S_{11}(\mathbf{p}, f_i)|$ is the response from the FEM forward solution at the frequency f_i , and $|\bar{S}_{11}(f_i)|$ is the target response. We use Matlab's fmincon optimisation algorithm, which uses a trust region and sets the initial trust region radius automatically. The evolution of the objective function and the parameter step size against iterations are shown in Figs. 8 and 9.

We use the FD-SASA and B/FD-SASA methods to supply the Jacobian to the optimisation algorithm. The initial guess of the shape parameters is $\mathbf{p}^{(0)} [w \ l \ d] [40 \ 40 \ 20]$ (in mm) with both methods. Both FD-SASA and B/FD-SASA result in an optimisation, which takes 8 iterations to converge to an optimal point. The optimal point with the FD-SASA is $x_{\text{FD-SASA}}^{*(8)} = [42.8 \ 57.7 \ 5.51]$ (in mm), while that of the B/FD-SASA is $x_{\text{B/FD-SASA}}^{*(8)} = [44.2 \ 54.1 \ 5.97]$ (in mm). The B/FD-SASA switches to the FD-SASA method once at the 4th iteration. The CPU time required by the optimisation using FD-SASA and B/FD-SASA is 7328 and 4330 s, respectively. Thus, the B/FD-SASA optimisation is about 1.7 times faster than the FD-SASA one. The computational gain increases as the number of optimisable parameters increases and the size of the FEM system matrix increases [11].

4.2 Validation with the method of moments

We consider the stacked probe-fed printed annular ring antenna of [24], which is shown in Fig. 10. The simulations are performed with the commercial simulator FEKO [25]

Table 1: Optimal designs using different sensitivity analysis methods with TR-minimax

	L_1	L_2	L_3	W_1	W_2	W_3	W_4
FD (mm)	12.226	14.042	17.483	14	11	10.922	11.341
FD-SASA (mm)	12.233	14.088	17.485	14	11	10.987	11.378
Mixed B/FD-SASA (mm)	12.131	13.855	17.809	14.01	11.1	11.098	11.191

Table 2: Number of iterations and time comparison between the different optimisation methods

	TR-Minimax			SQP-Minimax		
	FD	FD-SASA	B/FD-SASA	FD	FD-SASA	B/FD-SASA
Optimization iterations	11	11	9	8	8	6
Calls for EM simulation	88	11	9	312	39	55
Response computation (s)	473	473	387	1677	1677	2365
Jacobian estimation (s)	3311	1892	524	11 739	6708	2934
Total optimisation time (s)	3825	2403	949	13 561	8523	5479

Notes: (i) The EM simulator requires ~ 43 s to compute the field and the S -parameters. (ii) TR-Minimax calls the simulator once per optimization iteration. (iii) SQP-Minimax calls the simulator many times per optimization iteration

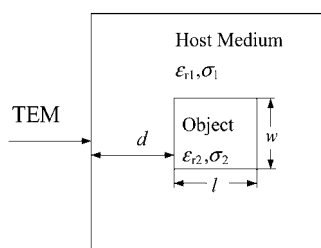
based on the MoM. The antenna is printed on a printed circuit board (PCB) with $\epsilon_{r1} = 2.2$, $d_1 = 6.096$ mm for the lower substrate, and $\epsilon_{r2} = 1.07$, $d_2 = 8.0$ mm for the upper substrate. The dielectric loss tangent is 0.001 for both layers. The radius of the feed pin is $r_0 = 0.325$ mm. The design variables are the outer and inner radius of each ring and the feed position, namely, $\mathbf{p} = [a_1 \ a_2 \ b_1 \ b_2 \ \rho_p]^T$. The design specification is

$$|S_{11}| \leq -10 \text{ dB} \quad \text{for} \quad 1.75 \leq f \leq 2.15 \text{ GHz.}$$

We supply the Jacobian calculated by our B/FD-SASA and FD-SASA techniques to the TR-minimax optimisation algorithm. The initial trust-region size is set to $r_0 = 0.05 \cdot \|\mathbf{p}^{(0)}\|_2$. The starting point is $\mathbf{p}^{(0)} = [a_1 \ a_2 \ b_1 \ b_2 \ \rho_p = [30 \ 30 \ 20 \ 10 \ 10]$ (in mm). The reflection $|S_{11}|$ of the initial design is plotted in Fig. 11.

The B/FD-SASA algorithm switches to FD-SASA three times at the 4th, 9th and 10th iterations. Both approaches converge within 11 iterations. The optimal designs emerge as $\mathbf{p}_{\text{B/FD-SASA}}^{*(11)} = [33.139 \ 28.836 \ 18.592 \ 9.9592 \ 8.8593]$ (in mm) and $\mathbf{p}_{\text{FD-SASA}}^{*(11)} = [33.088 \ 28.992 \ 18.437 \ 9.849 \ 8.5712]$ (in mm). For comparison, their responses are plotted in Fig. 11.

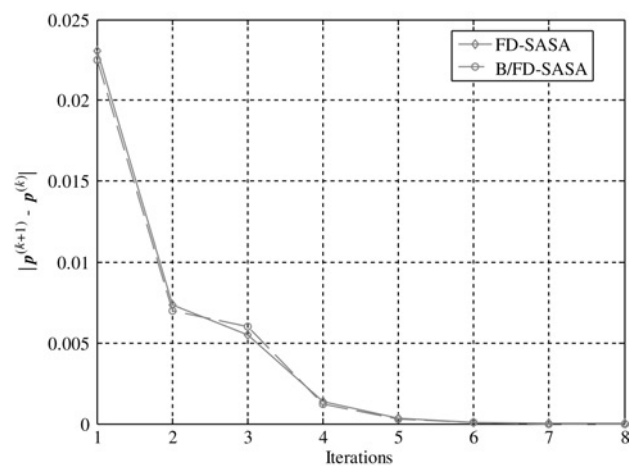
Figs. 12 and 13 show the parameter step size and the objective function against iterations, respectively. From Figs. 11–13, it is clear that both designs are practically identical. The overall time cost for the optimisation with the B/FD-SASA is 2115 s against 4358 s for the FD-SASA optimisation. Again, significant time saving is observed.

**Fig. 7** 2-D inverse imaging problem

5 Software requirements: mesh control and the system matrix

The Broyden update of the FEM and MoM system matrix derivatives requires that the mesh topology is preserved from one optimisation iteration to another. This ensures that the matrix size and the numbering of the mesh nodes and edges are preserved – the mesh is only locally stretched or shrunk.

In general, the global coordinates of the nodes as well as the length and orientation of the edges of the topologically fixed mesh change when shape parameters change; however, these changes are neither introducing new state variables nor eliminating existing state variables. With in-house solvers, such mesh control can be easily realised. With commercial simulation packages, advanced mesh-control features must be used. For example, with FEKO, restrictions can be imposed locally on a segment of the structure [26]. This feature is referred to as “local meshing”. An example is shown in Fig. 14 where a printed ring is meshed via four concentric circular bands of triangular elements. There, the number of mesh edges along the five circular contours (thick lines) is topologically fixed at 13,

**Fig. 8** Parameter step size against optimisation iterations using the least-squares algorithm in the 2-D inverse problem

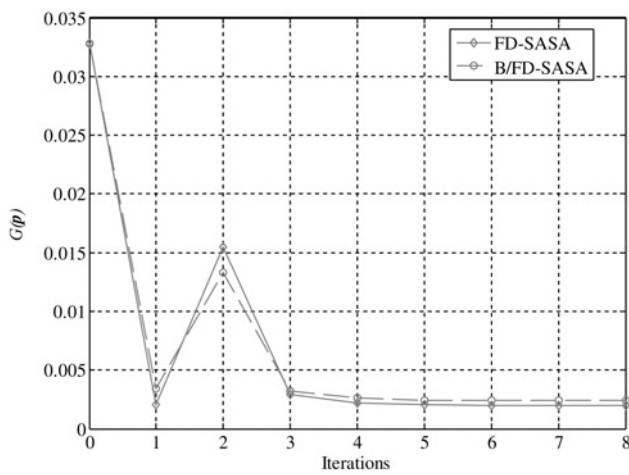


Fig. 9 Objective function against optimisation iterations using the least-squares algorithm in the 2-D inverse problem

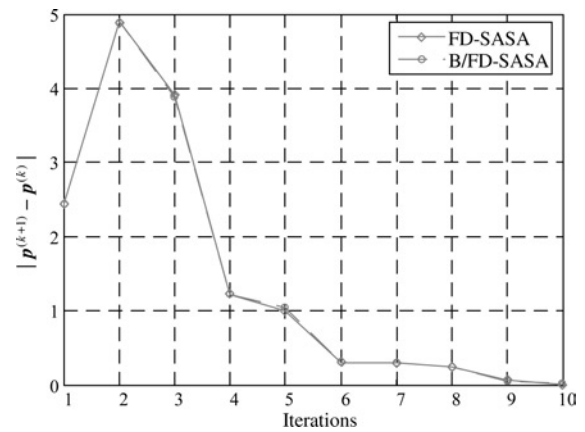


Fig. 12 Parameter step size against optimisation iterations using TR-minimax in the double annular ring example

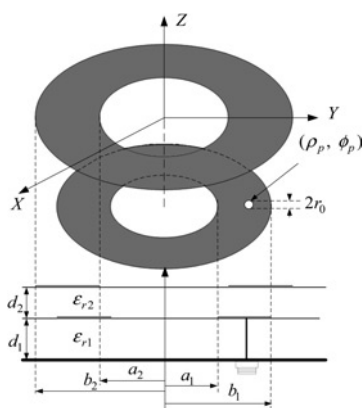


Fig. 10 Geometry of a stacked probe-fed printed double annular ring antenna

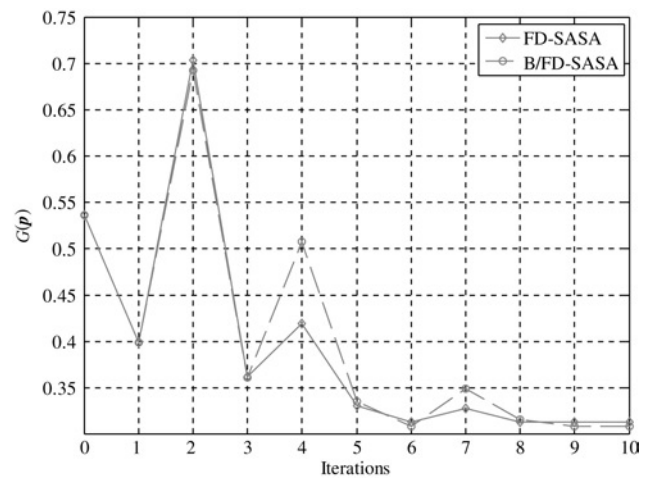


Fig. 13 Objective function against optimisation iterations using TR-minimax in the double annular ring example

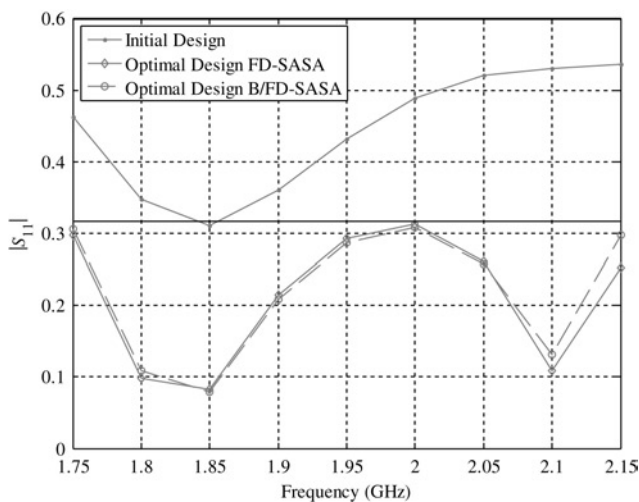


Fig. 11 Responses at the initial design and the optimal designs in the double annular ring example

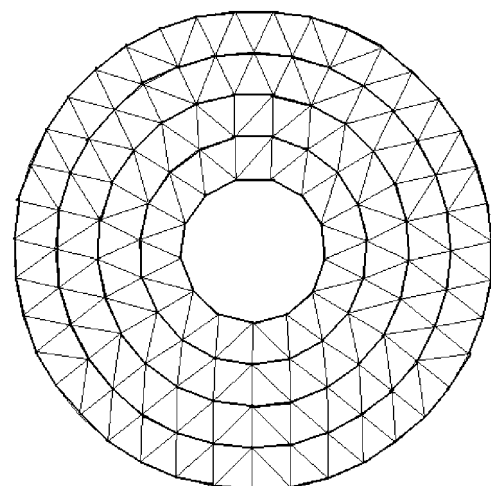


Fig. 14 Demonstration of local meshing of the stacked probe-fed printed double ring antenna

19, 25, 32 and 39, respectively. While the inner and outer radii of the printed ring change during the optimisation process, the mesh topology remains the same. With FEMLAB, the local mesh control is realised through the manipulation of the exported mesh file, that is, the file

which contains the coordinates of all mesh nodes of the initial structure. At each design iteration, the optimisable parameters change and the coordinates of affected mesh nodes are adjusted automatically, thereby generating a new mesh file for the next system analysis.

In addition to the mesh control, the FD-SASA requires access to the system matrix so that the system matrix derivatives can be computed [11]. Since B-SASA is initialised with a finite difference set of matrix derivatives, it has the same requirement. While most FEM and many MoM-based commercial EM solvers allow user-defined mesh control, only few of them give access to the system matrix. This is the reason why the examples presented here have been implemented in FEMLAB and FEKO – both packages allow the system matrix export.

6 Conclusions

We have proposed an efficient and practical approach to gradient-based EM optimisation. The proposed hybrid sensitivity analysis technique (B/FD-SASA) exploits self-adjoint sensitivities and Broyden's update at the level of the system matrix. It reduces the time cost of the optimisation significantly because of the reduced overhead of the sensitivity computation. The reduction is significant when compared with the optimisation exploiting response-level sensitivities as well as the optimisation exploiting our original FD-SASA approach, where finite differences are used to compute the system matrix derivatives. We also observe that often the optimisation algorithms exploiting the B/FD-SASA require fewer iterations to converge. At the same time, the optimisation results are nearly the same as those obtained by the optimisation algorithms based on either the FD-SASA or the finite-difference response level approximation. The time savings depend on the optimisation algorithms, as well as the numerical size of the problem. For electrically large 3-D problems with many design parameters, the time savings become significant.

The proposed approach is feasible for users of commercial MoM- and FEM-based simulators provided that (i) local mesh control is possible and (ii) the system matrix is accessible. Its potential, however, can be fully realised through direct incorporation within existing CAD packages where the mesh parameters and the system matrix are fully accessible.

7 References

- Belegundu, A.D., and Chandrupatla, T.R.: 'Optimisation concepts and applications in engineering optimisation' (Prentice Hall, Upper Saddle River, NJ, 1999)
- Neittaanmäki, P., Rudnicki, M., and Savini, A.: 'Inverse problems and optimal design in electricity and magnetism' (Oxford University Press, New York, 1996)
- Vogel, C.R.: 'Computational methods for inverse problems' (SIAM, Philadelphia, PA, 2002)
- Haug, E.J., Choi, K.K., and Komkov, V.: 'Design sensitivity analysis of structural systems' (Academic Press, Orlando, FL, 1986)
- Cacuci, D.G.: 'Sensitivity and uncertainty analysis, Vol. 1: theory' (Chapman and Hall/CRC, Boca Raton, FL, 2003)
- Arridge, S.R., and Schweiger, M.: 'Photon-measurement density functions. Part 2: finite-element-method calculations', *Appl. Optics*, 1995, **34**, (34), pp. 8026–8037
- Webb, J.P.: 'Design sensitivity of frequency response in 3-D finite-element analysis of microwave devices', *IEEE Trans. Magnet.*, 2002, **38**, (2), pp. 1109–1112
- Fang, Q., Meaney, P.M., Geimer, S.D., Streltsov, A.V., and Paulsen, K.D.: 'Microwave image reconstruction from 3-D fields coupled to 2-D parameter estimation', *IEEE Trans. Med. Imaging*, 2004, **23**, (4), pp. 475–484
- Fang, Q., Meaney, P.M., and Paulsen, K.D.: 'Singular value analysis of the Jacobian matrix in microwave image reconstruction', *IEEE Trans. Antennas Propagat.*, 2006, **54**, (8), pp. 2371–2380
- Nikolova, N.K., Bakr, M.H., and Bandler, J.W.: 'Adjoint techniques for sensitivity analysis in high-frequency structure CAD', *IEEE Trans. Microwave Theory Tech.*, 2004, **52**, (1), pp. 403–419
- Nikolova, N.K., Zhu, J., Li, D., Bakr, M.H., and Bandler, J.W.: 'Sensitivity analysis of network parameters with electromagnetic frequency-domain simulators', *IEEE Trans. Microwave Theory Tech.*, 2006, **54**, (2), pp. 670–681
- Nikolova, N.K., Li, Y., Li, Y., and Bakr, M.H.: 'Sensitivity analysis of scattering parameters with electromagnetic time-domain simulators', *IEEE Trans. Microwave Theory Tech.*, 2006, **54**, (4), pp. 1598–1610
- Georgieva, N.K., Glavic, S., Bakr, M.H., and Bandler, J.W.: 'Feasible adjoint sensitivity technique for EM design optimisation', *IEEE Trans. Microwave Theory Tech.*, 2002, **50**, (12), pp. 2751–2758
- Broyden, C.G.: 'A class of methods for solving nonlinear simultaneous equations', *Math. Comput.*, 1965, **19**, (92), pp. 577–593
- Bandler, J.W., Chen, S.H., Daijavad, S., and Madsen, K.: 'Efficient optimisation with integrated gradient approximations', *IEEE Trans. Microwave Theory Tech.*, 1988, **36**, (2), pp. 444–455
- Nikolova, N.K., Safian, R., Soliman, E.A., Bakr, M.H., and Bandler, J.W.: 'Accelerated gradient based optimisation using adjoint sensitivities', *IEEE Trans. Antennas Propagat.*, 2004, **52**, (8), pp. 2147–2157
- Soliman, E.A., Bakr, M.H., and Nikolova, N.K.: 'Accelerated gradient-based optimisation of planar circuits', *IEEE Trans. Antennas Propagat.*, 2005, **53**, (2), pp. 880–883
- Jin, J.: 'The finite element method in electromagnetics' (John Wiley and Sons, New York, 2002, 2nd edn.), pp. 496–497
- FEMLAB[®] 3.1 User's Guide, 2004 COMSOL, Inc., 8 New England Executive Park, Suite 310, Burlington, MA 01803, USA, <http://www.comsol.com>
- Matthaei, G., Young, L., and Jones, E.M.T.: 'Microwave filters, impedance-matching networks, and coupling structures' (Artech House, Norwood, MA, 1980), pp. 545–547
- Bandler, J.W., Kellerman, W., and Madsen, K.: 'A superlinearly convergent minimax algorithm for microwave circuit design', *IEEE Trans. Microwave Theory Tech.*, 1985, **33**, (12), pp. 1519–1530
- Dennis, J.E., and Schnabel, R.B.: 'Numerical methods for unconstrained optimisation and nonlinear equations' (Prentice Hall, Englewood Cliffs, NJ, 1983)
- Sartenaer, A.: 'Automatic determination of an initial trust region in nonlinear programming', *SIAM J. Sci. Comput.*, 1997, **18**, (6), pp. 1788–1803
- Kokotoff, D.M., Aberle, J.T., and Waterhouse, R.B.: 'Rigorous analysis of probe-fed printed annular ring antennas', *IEEE Trans. Antennas Propagat.*, 1999, **47**, (2), pp. 384–388
- FEKO[®] User's Manual, Suite 4.2, June 2004, EM Software and Systems-S.A. (Pty) Ltd, Stellenbosch, South Africa, <http://www.feko.info>. In the USA: EM Software and Systems (USA), Inc., Hampton, VA 23666, USA, <http://www.emssusa.com/>
- 'Mesh refinement', FEKO Quarterly, December 2004